AIP | Applied Physics Letters

Microscopic energy conversion process in the ion drift region of electrohydrodynamic flow

Chul Kim, Kwang-Chul Noh, Junho Hyun, Sang-Gu Lee, Jungho Hwang et al.

Citation: Appl. Phys. Lett. **100**, 243906 (2012); doi: 10.1063/1.4729443
View online: http://dx.doi.org/10.1063/1.4729443
View Table of Contents: http://apl.aip.org/resource/1/APPLAB/v100/i24
Published by the American Institute of Physics.

Microscopic energy conversion process in the ion drift region of electrohydrodynamic flow

Chul Kim,[1,a)] Kwang-Chul Noh,[1] Junho Hyun,[2] Sang-Gu Lee,[2] Jungho Hwang,[1,2,b)] and Hiki Hong[3]
[1]*School of Mechanical Engineering, Yonsei University, 134 Sinchon-dong, Seodaemun-ku, Seoul 120-749, South Korea*
[2]*Graduate Programs in Clean Technology, Yonsei University, 134 Sinchon-dong, Seodaemun-ku, Seoul 120-749, South Korea*
[3]*Department of Mechanical Engineering, Kyung Hee University, Yongin 446-701, South Korea*

(Received 13 April 2012; accepted 29 May 2012; published online 15 June 2012)

We theoretically investigated the momentum transfer and energy conversion process of ion-neutral and ensuing neutral-neutral collisions in the ion drift region of electrohydrodynamic flow. Our results are presented in explicit equations with physical interpretations of the phenomena. The unit conversion process was estimated to sustain for 1.0 nano-second in a very tiny 0.5-μm-sized volume in the air. Also, the continuum-based equation formulations are presented according to the microscopic energy conversion phenomena. Numerical simulations reflecting those formulations are performed to verify the theoretical results and experimentally supported by an air corona discharge. © *2012 American Institute of Physics*. [http://dx.doi.org/10.1063/1.4729443]

In a point-to-plane corona discharge, a small ionization region with high electric field is formed around the point, where chemical energy conversion process (ionization, ozone formation, etc.) occurs.[1,2] On the other hand, in the unipolar ion drift region connected in series with the ionization region between the point and the plate,[1,2] ions acquire momentum and energy from the applied electric field and transfer them to the surrounding neutral molecules through ion-neutral collisions, consequently, inducing an EHD (electrohydrodynamic) flow.[3–8] This molecular collision process in the ion drift region generates a thrust, and a reactive air flow called an ionic wind, that can be applied for flow control[4,5] and electric propulsion.[6,8–10] Most previous studies for this process agree on the fundamental phenomenon: ion-neutral collision. However, they show much disagreement about the explicit equations representing the electric-to-kinetic energy conversion efficiency, η_K. η_K was expressed in different equations as the function of macroscopic parameters (applied voltage, current, electrode distance, corona initiation voltage, fluid density, ion mobility, permittivity, etc.) in the 1960s[3,8,11] and in 1985.[2] Bondar and Bastien[12] conceptually formulated η_K using only fluidic parameters as $\eta_K = 1/(1 + U_d/U_a)$, where U_d is the ion drift velocity and U_a is the neutral fluid velocity. Other studies have presented $\eta_K = U_a/(2U_d)$,[13] and $\eta_K = \sqrt{\varepsilon_o/\mu}$,[14] where ε_o is the air permittivity and μ is the ion mobility. These disagreements are thought to have occurred because all these equations were formulated based on continuum mechanics with different assumptions for the macroscopic conditions without a clear understanding of ion-neutral collision. In this paper, we try to understand the molecular energy conversion process in the ion drift region for just one ion-neutral collision and the following neutral-neutral collisions. We derive the theoretical equations representing this microscopic conversion process. Also, we provide physical interpretations for the energy conversion phenomena and continuum-based formulations based on microscopic analysis.

Figure 1 illustrates a schematic microscopic energy conversion process in the EHD flow. The average three-dimensional translational velocity of an ion should be the same as the macroscopic ion velocity $\mathbf{U}_d + \mathbf{U}_a$ (the ion drift velocity $\mathbf{U}_d = \mu\mathbf{E}$, where $\mathbf{E}$ is the applied electric field and $\mathbf{U}_a$ is the convective fluid velocity). The ion acquires the average translational momentum $\mathbf{f} \cdot \Delta t$ and the average translational kinetic energy $\mathbf{f} \cdot \Delta\mathbf{l}$ between the successive ion-neutral collisions from $\mathbf{E}$, where $\mathbf{f}$ is the Coulomb's force $q_i\mathbf{E}$ (q_i: ion charge quantity, Δt: mean travel time, $\Delta\mathbf{l}$: mean travel distance). In this paper, we refer to the translational momentum and the translational kinetic energy as the momentum and the kinetic energy, respectively. Hence, the electrical input energy into an ion can be expressed as follows by using $\Delta\mathbf{l} = (\mathbf{U}_d + \mathbf{U}_a)\Delta t$ relation:

$$\mathbf{f} \cdot \Delta\mathbf{l} = \frac{q_i}{\mu}\mathbf{U}_d \cdot (\mathbf{U}_a + \mathbf{U}_d)\Delta t. \tag{1}$$

This equation implies that the electrical energy supplied to the ion can be decomposed into the kinetic energies caused by $\mathbf{U}_a$ and $\mathbf{U}_d$. If we assume the ion-neutral collision is elastic, $\mathbf{f} \cdot \Delta t$ and $\mathbf{f} \cdot \Delta\mathbf{l}$ are transferred from the ion to the neutral through each ion-neutral collision ($s = 0$ in Fig. 1). The neutral molecule moves to the right with the increased momentum $\mathbf{f} \cdot \Delta t$ and the increased kinetic energy $\mathbf{f} \cdot \Delta\mathbf{l}$. Subsequently, it collides with other neutral ($s = 1$ in Fig. 1). This first neutral-neutral collision following the ion-neutral collision triggers one more neutral to move to the right by transferring some portion of $\mathbf{f} \cdot \Delta t$ and $\mathbf{f} \cdot \Delta\mathbf{l}$ ($s = 2$ in Fig. 1), and subsequently two neutrals trigger 4 molecules to move to the right ($s = 3$ in Fig. 1), and so on (dissipation zone in Fig. 1). Finally, all the neutrals influenced by the ion-neutral collisions, henceforth denoted as a colony in this paper, will smear out into the overall flow motion $\mathbf{U}_a$ (conservation

[a)]Electronic mail: kalsoo1@msn.com.
[b)]Electronic mail: hwangjh@yonsei.ac.kr.

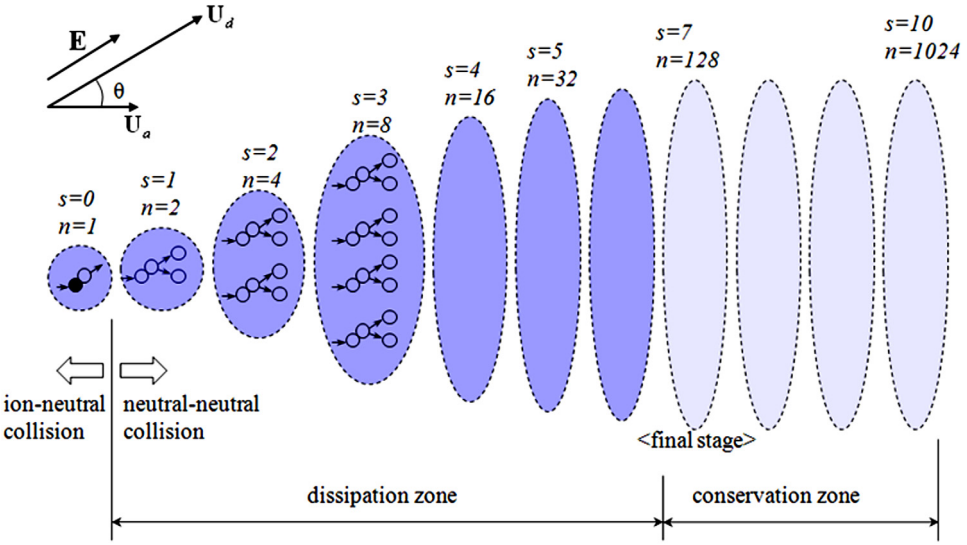

FIG. 1. Microscopic energy conversion process in the EHD flow. ●: ion ○: neutral molecule. One colony (grouped neutrals in a shaded oval enclosed by the dashed line) is born from an ion-neutral collision and drifts to the right. It evolves (heavy ovals, dissipation zone) and gradually smears out (light ovals, conservation zone) into the surrounding EHD flow. The number of colony neutrals influenced by the initial ion-neutral collision are doubled ($n=1, 2, 4, 8\ldots$) in accord with each collision stage ($s=0, 1, 2, 3\ldots$) as time passes, $n=2^s$. Schematic collision diagrams are shown only for $s=0$ to 3 and not shown for $s>3$. All the ovals are considered as spheres in the actual three dimensional space. Upper left diagram: $\mathbf{U}_d$ (average ion drift velocity) and $\mathbf{E}$ (electric field) make an angle θ with $\mathbf{U}_a$ (average fluid velocity).

zone in Fig. 1). We assume that the ion and the neutrals have the same mass m. The total kinetic energy e_k of one molecule can be expressed as $e_k=\frac{1}{2}mU^2+\frac{3}{2}kT$, where U is the translational velocity, k is the Boltzmann constant, and T is the temperature (K).[15] $\mathbf{f}\cdot\Delta t$ and $\mathbf{f}\cdot\Delta\mathbf{l}$ should be conserved through all these elastic neutral (colony member)-neutral (non-colony member) collisions. We can express the momentum and energy conservations for the colony members in the final stage of Fig. 1 as follows:

$$\mathbf{f}\cdot\Delta t+n_f m\mathbf{U}_a=n_f m(\mathbf{U}_a+\Delta\mathbf{U}_a), \tag{2}$$

$$\mathbf{f}\cdot\Delta\mathbf{l}+n_f\frac{1}{2}m\mathbf{U}_a\cdot\mathbf{U}_a+n_f\frac{3}{2}kT_a = n_f\frac{1}{2}m(\mathbf{U}_a+\Delta\mathbf{U}_a)\cdot(\mathbf{U}_a+\Delta\mathbf{U}_a)+n_f\frac{3}{2}kT_f, \tag{3}$$

where n_f is the number of colony members, $\Delta\mathbf{U}_a$ is the average velocity increment of the colony members in the final stage colony, and T_a and T_f are, respectively, the temperatures before and after becoming colony members. $n_f m\mathbf{U}_a$ and $n_f\frac{1}{2}m\mathbf{U}_a\cdot\mathbf{U}_a$ represent the momentum and the kinetic energy of the neutrals before they become the colony members, respectively. $n_f m(\mathbf{U}_a+\Delta\mathbf{U}_a)$ and $n_f\frac{1}{2}m(\mathbf{U}_a+\Delta\mathbf{U}_a)\cdot(\mathbf{U}_a+\Delta\mathbf{U}_a)$ represent the momentum and kinetic energy after they become colony members. From Eq. (3), the kinetic energy increment $\Delta E_K\left(=n_f\frac{1}{2}m(\mathbf{U}_a+\Delta\mathbf{U}_a)\cdot(\mathbf{U}_a+\Delta\mathbf{U}_a)-n_f\frac{1}{2}m\mathbf{U}_a\cdot\mathbf{U}_a\right)$ conserved in the final stage colony leads to the following simple form by using a relation $\mathbf{f}\cdot\Delta t=n_f m\Delta\mathbf{U}_a$ deduced from Eq. (2), $\mathbf{U}_d=\mu\mathbf{E}$ and $\mathbf{f}=q_i\mathbf{E}$ relations, and neglecting $\Delta\mathbf{U}_a\cdot\Delta\mathbf{U}_a$, because $\Delta\mathbf{U}_a$ is very small:

$$\Delta E_K=\frac{q_i}{\mu}\mathbf{U}_d\cdot\mathbf{U}_a\Delta t. \tag{4}$$

Using an additional relation, $\Delta\mathbf{l}=(\mathbf{U}_d+\mathbf{U}_a)\Delta t$, the thermal energy increment $\Delta E_T\left(=n_f\frac{3}{2}kT_f-n_f\frac{3}{2}kT_a\right)$ in the final stage colony is reduced from Eq. (3) as follows:

$$\Delta E_T=\frac{q_i}{\mu}\mathbf{U}_d\cdot\mathbf{U}_d\Delta t. \tag{5}$$

Hence, the electrical to kinetic energy conversion efficiency $\eta_K(=\Delta E_K/\mathbf{f}\cdot\Delta\mathbf{l})$ and the electrical to thermal energy conversion efficiency $\eta_T(=\Delta E_T/\mathbf{f}\cdot\Delta\mathbf{l})$ are expressed as the following equations:

$$\eta_K=\frac{\mathbf{U}_d\cdot\mathbf{U}_a}{\mathbf{U}_d\cdot(\mathbf{U}_d+\mathbf{U}_a)}, \tag{6}$$

$$\eta_T=\frac{\mathbf{U}_d\cdot\mathbf{U}_d}{\mathbf{U}_d\cdot(\mathbf{U}_d+\mathbf{U}_a)}. \tag{7}$$

The above two equations become $\eta_K=U_a/(U_d+U_a)$ and $\eta_T=U_d/(U_d+U_a)$ when $\theta=0^\circ$ (see Fig. 1).

In the above neutral-neutral collisions in the dissipation zone, the thermal velocity $\mathbf{U}_T(\frac{3}{2}kT=\frac{1}{2}m|\mathbf{U}_T|^2)$ is included in the actual three-dimensional motions. Without loss of generality, this complicated state can be transformed into a binary collision system:[16] the colony molecule is a projectile with a velocity $\mathbf{U}_p$ ($|\Delta\mathbf{U}_a|\le|\mathbf{U}_p|\le|\mathbf{U}_d|$), and the target is the stationary non-colony molecule. In this collision system, the average energy loss fraction of the projectile is 1/2 per each collision.[16] Hence, the first colony neutral (which experienced the ion-neutral collision) exhibits a kinetic energy lower than 1% of the initial value after undergoing 7 consecutive collision stages ($s=1$ through $s=7$, Fig. 1). If we take this 1% of the energy level as the criteria for the final stage, the final stage colony is composed of 128 ($=2^7$) neutrals, and they experience 1 to 7 collisions in the chain collision process. In standard air conditions (mean free path: 0.066 μm, mean thermal velocity: 462.9 m/s at 20 °C),[17] we can roughly estimate the average process time (the survival time of a colony) as 1.0 nano-second ($0.066\,\mu\text{m}\times 7/462.9\,\text{m/s}$) and the average colony size as 0.5μm ($0.066\,\mu\text{m}\times 7$). Considering that the actual velocity of a

colony neutral ($\mathbf{U}_T + \mathbf{U}_p$) is greater than the thermal velocity $\mathbf{U}_T$ of a non-colony neutral, the average process time should be shorter than 1.0 nano-second. In this regard, the microscopic energy conversion process can be said to be an almost instantaneous phenomenon occurring in a very tiny volume. This suggests that we can treat the energy conversion process on a continuum basis.

As a physical interpretation of the above microscopic process, a comparison of the electrical input energy into an ion (Eq. (1)) with the energy conversion results (Eqs. (4) and (5)) suggests that the electric energy input caused by the fluid velocity $\mathbf{U}_a$ is conserved in the flow, while the other portion caused by the ion drift velocity $\mathbf{U}_d$ is dissipated into thermal energy through neutral-neutral collisions. This mechanism can be used for the continuum based energy conversion formulation. Consider a very small volume $\Delta\upsilon$ (which includes at least one colony) drifting in 3-dimensional space with unipolar charge density q when the electric field is $\mathbf{E}$. The Coulomb's force exerted on this volume is $\Delta\mathbf{F} = q\mathbf{E}\Delta\upsilon$ so that the electric power input into this volume is $q\mathbf{E}\cdot(\mathbf{U}_d + \mathbf{U}_a)\Delta\upsilon$ (corresponding to Eq. (1)). The conversion rates (W/m^3) into the kinetic energy and the thermal energy are $q\mathbf{E}\cdot\mathbf{U}_a\Delta\upsilon$ (corresponding to Eq. (4)) and $q\mathbf{E}\cdot\mathbf{U}_d\Delta\upsilon$ (corresponding to Eq. (5)), respectively. However, some portion of $q\mathbf{E}\cdot\mathbf{U}_a\Delta\upsilon$ should be converted into thermal energy due to the fluid dissipation process,[18] which is independent of the above colony process. This quantity can be expressed as $\varepsilon_f\Delta\upsilon$ (ε_f: fluidic dissipation rate). Therefore, the above 4 equations in order can be expressed as the integral forms in the whole domain: $\int_\upsilon q\mathbf{E}\cdot(\mathbf{U}_d + \mathbf{U}_a)\Delta\upsilon$, $\int_\upsilon q\mathbf{E}\cdot\mathbf{U}_a\Delta\upsilon$, $\int_\upsilon q\mathbf{E}\cdot\mathbf{U}_d\Delta\upsilon$, $\int_\upsilon \varepsilon_f\Delta\upsilon$, and overall η_K and η_T are expressed as follows:

$$\eta_K = \frac{\int_\upsilon (q\mathbf{E}\cdot\mathbf{U}_a - \varepsilon_f)d\upsilon}{\int_\upsilon q\mathbf{E}\cdot(\mathbf{U}_d + \mathbf{U}_a)d\upsilon}, \tag{8}$$

$$\eta_T = \frac{\int_\upsilon (q\mathbf{E}\cdot\mathbf{U}_d + \varepsilon_f)d\upsilon}{\int_\upsilon q\mathbf{E}\cdot(\mathbf{U}_d + \mathbf{U}_a)d\upsilon}. \tag{9}$$

Under the conditions of constant θ, $|\mathbf{U}_a| \ll |\mathbf{U}_d|$, and negligible ε_f, Eq. (8) leads to the relation, $\eta_K \propto \frac{\bar{U}_a}{\bar{U}_d}$, which was experimentally proven by Kim *et al.* (Ref. 19).

We performed an experiment to verify the proposed energy conversion process in a wire-to-converging plate corona discharge configuration[7] (Fig. 2(a)) in air, and a numerical simulation reflecting above formulations was performed (Figs. 2(b)–2(f)). The two-dimensional Poisson equation and the charge conservation equations coupled with the continuity and momentum equations were solved using Fluent according to our previous studies (Refs. 10 and 20). In this paper, we additionally solved an energy equation where the thermal energy conversion rate $q\mathbf{E}\cdot\mathbf{U}_d + \varepsilon_f$ was used as the energy source distributed in the whole domain. As shown in Fig. 2(b), the tilted collector configuration produces denser electric lines in the right side of the emitter, which indicates a stronger electric field, so that Coulombic body force to the right side with respect to the emitter is higher than the one to the left side (Fig. 2(c)). Consequently, this results in a weak air flow to the right (Fig. 2(d)). Unbalanced body force distribution generates a swirl in the left side of the emitter. The thermal energy conversion rate $q\mathbf{E}\cdot\mathbf{U}_d$ (Fig. 2(e)) produced the temperature profiles as shown in Fig. 2(f) due to the air flow directed from the inlet to the outlet.

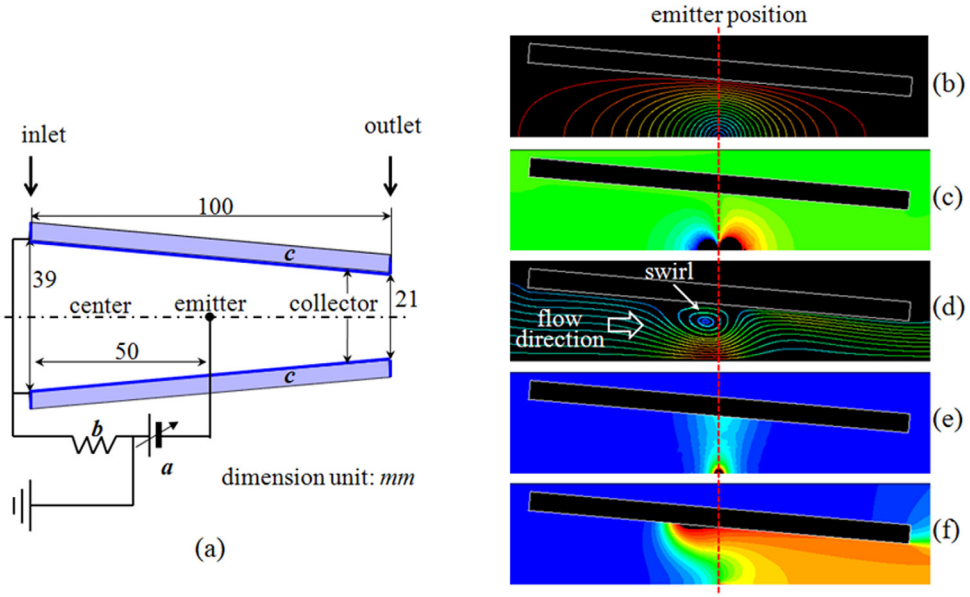

FIG. 2. (a) Schematic cross-section of horizontal experiment set-up. (b)–(f) Simulation results corresponding to (a) for applied voltage − 10 kV, current 0.576 mA, where only the partial upper half domain is shown out of the total calculation domain (symmetrical with respect to the center, width 350 mm, height 100 mm). ***a***: high voltage power supply (ULTRAVOLT, 15A24-N30), ***b***: shunt resistor (100 kΩ, used for current measurement), ***c***: insulator. Rig width (length of emitter and collectors): 200 mm, emitter: diameter 0.04 mm (tungsten wire). Collector (aluminum foil) was attached on the insulator (Styrofoam, 5 mm thickness) surface in order to minimize the heat transfer into the collector. (b) electric potential lines (red: 150 V, blue: −10 kV), (c) body force in the flow direction (blue: − 300 N/m^3, yellowish green: 0 N/m^3, red: 300 N/m^3, blue (negative value) and red (positive value) mean the forces to the left and the right, respectively), (d) path-lines of air flow with velocity (blue: 0 m/s, red: 1.4 m/s), (e) thermal energy conversion rate (blue: 0 W/m^3, red: 200 000 W/m^3), (f) profiles of temperature rise with respect to the ambient inlet temperature (blue: 0 °C, red: 2.0 °C). The viscous model for the simulation is turbulent (Reynolds stress).

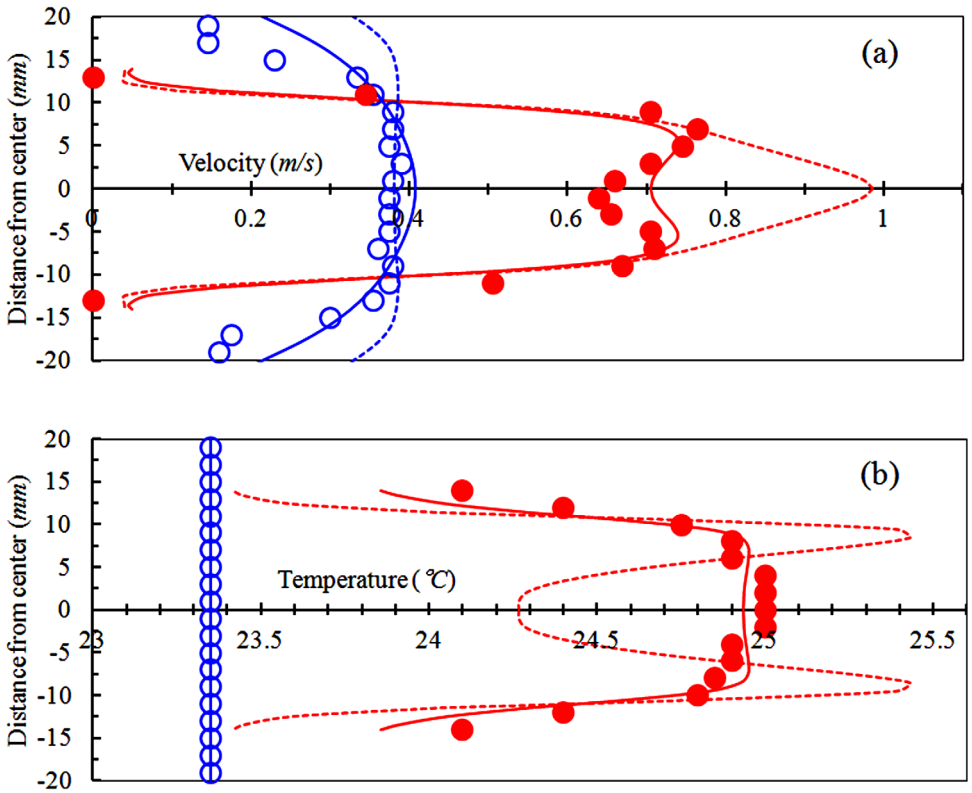

FIG. 3. (a) Velocity profiles, (b) temperature profiles in the inlet (blue) and the outlet (red). Inlet temperature: 23.35 °C. Electrical conditions; ⟨Experiment⟩ applied voltage = −10 kV (negative discharge) current = 0.589 mA, ⟨Simulation⟩ applied voltage = −10 kV current = 0.576 mA. ●: outlet experimental data, ○: inlet experimental data, solid line (—): simulation result (turbulent flow, Reynolds-stress model), and dashed line (. . .): simulation result (laminar flow). Measurements were made 5 mm above the collector plate tip (outlet) and 5 mm below the collector plate tip (inlet) in the middle of the rig by vertically moving the probes at 2 mm intervals. Velocity measurement by a hot-wire anemometer (TSI, model 8330-M-GB, resolution 0.01 m/s), temperature measurement by a digital thermometer (testo, model 735-1, Pt sensor, resolution 0.05 °C). Relative humidity: 39.5–40.0%.

The experimental current 0.589 mA was almost identical to the simulation current 0.576 mA (0.576/0.589 = 0.98) when $\mu = 2.0 \times 10^{-4} \mathrm{m}^2/\mathrm{V} \cdot \mathrm{s}$.[1,9] Considering the simulated current density ($\mathbf{j} = q\mu\mathbf{E}$) in the discharge space and the current (integral of $\mathbf{j}$ on the collector surface), we can say that simulated q, $\mathbf{E}$ fields are almost the same as the experimental ones. Figure 3(a) reveals decent agreement between the experimental velocity and the simulated velocity both in the inlet and the outlet when the simulated flow is turbulent. Those results agree with the previous experimental conclusion for the same electrode configuration (Tsubone *et al.*;[7] *the flow was always turbulent or limited re-circulating laminar flow, M-shaped outlet velocity profile*). The agreement of velocities between the experiment and the simulation re-confirms that simulated q, $\mathbf{E}$ fields are similar to the experimental ones because we used Coulomb's force ($\mathbf{F} = q\mathbf{E}$) as the body force in the momentum equation in order to obtain the $\mathbf{U}_a$ field. Also, the above result suggests that the simulated $\mathbf{U}_a$ field in the discharge volume (a volume enclosed by the inlet, outlet and collectors) would be close to the experimental $\mathbf{U}_a$ field. In this regard, we presumed that the simulated total kinetic energy generation rate 0.00333 W ($\int_v q\mathbf{E} \cdot \mathbf{U}_a \Delta v$) would be close to the experimental one.

Figure 3(b) reveals good agreement between the experimental outlet temperature profile and the simulated one (turbulent). The macroscopic energy conversion process for the discharge volume can be written as follows for the steady state incompressible flow condition neglecting heat transfer to the collectors:

$$P_{in} \Rightarrow \int_v \mathbf{F} \cdot (\mathbf{U}_d + \mathbf{U}_a) dv$$

$$\Rightarrow \rho C_p \int_{A_o} U_o (T_o - T_i) dA + \frac{1}{2}\rho \left(\int_{A_o} {U_o}^3 dA - \int_{A_i} {U_i}^3 dA \right),$$

(P_{in}: electric input power, ρ: air density (1.204 kg/m^3 at 20 °C), C_p: constant pressure specific heat (1002.8 J/kg · K at 20 °C), A_o: outlet area, U_o: outlet velocity, T_o: outlet temperature, T_i: inlet temperature, A_i: inlet area, and U_i: inlet velocity). The above process was calculated as (P_{in}5.76 W ⇒ 5.72 W ⇒ 5.62 W + 0.00062 W) for the simulation and (P_{in}5.85 W ⇒ 5.79 W + 0.00067 W; we could not measure $\int_v \mathbf{F} \cdot (\mathbf{U}_d + \mathbf{U}_a) dv$) for the experiment. *The overwhelming part of the energy goes into gas heating in the corona discharge*.[2] Hence, we think that the similarity between 5.62 W and 5.79 W is essential in supporting the microscopic electric to thermal energy conversion process, even though we did not consider the electric to chemical energy conversion process in our simulation. Also, the agreement of 0.00062 W and 0.00067 W supports the electric to kinetic energy conversion process. Those values are lower than 0.00333 W ($\int_v q\mathbf{E} \cdot \mathbf{U}_a \Delta v$). We think the balance 0.00266 W (0.00333–0.00067 W) was converted to increase the pressure between the inlet and the outlet, or converted to thermal energy through the fluidic dissipation process. The experimental η_K in the previous studies[4,5,19] was evaluated by the definition: $\frac{1}{2}\rho \int_{A_o} {U_o}^3 dA$ over P_{in}, which was calculated as 0.0146% (0.000841 W/5.76 W) in our simulation and as 0.0147% (0.00086 W/5.85 W) in our experiment. These values are quite lower than the previous η_K values of about 1.0% (Refs. 3, 5, and 19) due to the high θ (close to 90°) in our case.

In conclusion, we propose a model for the microscopic energy conversion process in the EHD flow. Based on the model, we formulated microscopic-to-macroscopic equations describing this process, which were numerically and experimentally supported. We suppose that our model and approach method will be helpful in the investigations of electrical discharges in the flow field.

This research was supported by a grant (Grant No. 2010-0023098) from the National Research Foundation of Korea.

[1]R. S. Sigmond, J. Appl. Phys. **53**, 891 (1982).
[2]M. Goldman, A. Goldman, and R. S. Sigmond, Pure Appl. Chem. **57**, 1353 (1985).
[3]M. Robinson, Trans. Am. Inst. Electr. Eng. **80**, 143 (1961).
[4]E. Moreau, J. Phys. D: Appl. Phys. **40**, 605 (2007).
[5]D. F. Colas, A. Ferret, D. Z. Pai, D. A. Lacoste, and C. O. Laux, J. Appl. Phys. **108**, 103306 (2010).
[6]G. Makrinich and A. Fruchtman, Appl. Phys. Lett. **95**, 181504 (2009).
[7]H. Tsubone, J. Ueno, B. Komeili, S. Minami, G. D. Harvel, K. Urashima, C. Y. Ching, and J. S. Chang, J. Electrostat. **66**, 115 (2008).
[8]E. A. Christenson and P. S. Moller, AIAA J. **5**, 1768 (1967).
[9]J. Wilson, H. D. Perkins, and W. K. Thompson, "An investigation of ionic wind propulsion," NASA/TM 2009–215822, 2009.
[10]C. Kim, K. C. Noh, S.Y. Kim, and J. Hwang, Appl. Phys. Lett. **99**, 111503 (2011).
[11]O. M. Stuetzer, J. Appl. Phys. **31**, 136 (1960).
[12]H. Bondar and F. Bastien, J. Phys. D: Appl. Phys. **19**, 1657 (1986).
[13]R. S. Sigmond and I. H. Lagstadt, High Temp. Chem. Process. **2**, 221 (1993).
[14]T. I. J. Goodenough, P. W. Goodenough, and S. M. Goodenough, J. Food Eng. **80**, 1233 (2007).
[15]E. A. Mason and E. W. McDaniel, *Transport Properties of Ions in Gases* (Wiley, New York, 1987).
[16]M. A. Lieberman and A. J. Lichtenberg, *Principles of Plasma Discharges and Materials Processing*, 2nd ed. (Wiley, NJ, 2005).
[17]W. C. Hinds, *Aerosol Technology: Properties, Behavior, and Measurement of Airborne Particles*, 2nd ed. (Wiley, New York, 1998).
[18]S. B. Pope, *Turbulent Flows* (Cambridge University Press, New York, 2000).
[19]C. Kim, D. Park, K. C. Noh, and J. Hwang, J. Electrostat. **68**, 36 (2010).
[20]C. Kim, K. C. Noh, and J. Hwang, Aerosol Air Qual. Res. **10**, 446 (2010).